

# ChemComm

Accepted Manuscript



This is an *Accepted Manuscript*, which has been through the Royal Society of Chemistry peer review process and has been accepted for publication.

*Accepted Manuscripts* are published online shortly after acceptance, before technical editing, formatting and proof reading. Using this free service, authors can make their results available to the community, in citable form, before we publish the edited article. We will replace this *Accepted Manuscript* with the edited and formatted *Advance Article* as soon as it is available.

You can find more information about *Accepted Manuscripts* in the [Information for Authors](#).

Please note that technical editing may introduce minor changes to the text and/or graphics, which may alter content. The journal's standard [Terms & Conditions](#) and the [Ethical guidelines](#) still apply. In no event shall the Royal Society of Chemistry be held responsible for any errors or omissions in this *Accepted Manuscript* or any consequences arising from the use of any information it contains.



Journal Name

COMMUNICATION

## Exploration of calcium-organic framework as an anode material for sodium-ion batteries

Received 00th January 20xx,  
Accepted 00th January 20xx

Yan Zhang<sup>a,b</sup>, Yubin Niu<sup>a,b</sup>, Min-Qiang Wang<sup>a,b</sup>, Jingang Yang<sup>a,c</sup>, Shiyu Lu<sup>a,b</sup>, Jin Han<sup>a,b</sup>, Shu-Juan Bao<sup>a,b</sup>, Maowen Xu<sup>a,b\*</sup>

DOI: 10.1039/x0xx00000x

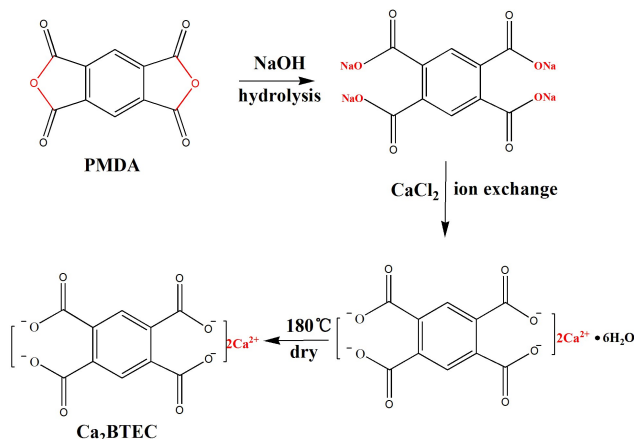
www.rsc.org/

In this communication, we designed and synthesized a novel calcium-organic framework and presented it as an anode material for sodium-ion batteries. The results show that it delivers reversible capacity of higher than 140 mA h g<sup>-1</sup> even after 300 cycles. The remarkable performance is attributed to the high structural stability and extremely low solubility of calcium-organic framework in the electrolytes.

Sodium-ion batteries (SIBs), as the most attractive alternative to lithium-ion batteries (LIBs), have gained extensive research attention owing to the low cost and abundant resource.<sup>1,2</sup> Similar to LIBs, most of host electrode materials in SIBs are inorganic compounds, such as transitional metal oxides,<sup>3,4</sup> polyanion compounds,<sup>5,6</sup> carbon materials<sup>7,8</sup> and alloy materials<sup>9,10</sup> et al. However, these materials are generally prepared through energy intensive processing from limited mineral resources, which enhanced the use cost greatly. Naturally, organic materials have come into our vision due to structural diversity and resource renewability.<sup>11</sup> Indeed, many organic-metal compounds have been studied as the novel electrode materials for LIBs and SIBs. However, these organic lithium/sodium salts electrodes suffer from serious capacity fading because of the solubility in organic electrolytes.<sup>12,13</sup> Fortunately, one approach using calcium instead of lithium in Li<sub>2</sub>C<sub>8</sub>H<sub>4</sub>O<sub>4</sub> to this issue was reported, due to its higher ionization energy with organic anions than that of Li<sup>+</sup>.<sup>14,15</sup> Meanwhile, Ca is an ample element widely distributed in the ocean and crust.<sup>16</sup> To our knowledge, reports have never been published to investigate the calcium displacement of sodium in organic sodium salts and its electrochemical behaviour in SIBs.

Herein, a novel calcium-organic framework (Ca<sub>2</sub>BTEC) composed of Ca<sup>2+</sup> and 1, 2, 4, 5-benzenetetracarboxylic acid

(H<sub>4</sub>BTEC) was designed and explored as an anode material for SIBs for the first time. Ca<sub>2</sub>BTEC delivered high capacity and excellent capacity retention. Ca<sub>2</sub>BTEC was synthesized by a facile hydrolysis and cationic exchange method. First, 1 mmol pyromellitic dianhydride (PMDA, Aladdin, 96%) and 4 mmol NaOH (Aladdin) were dissolved in 30 mL de-ionized water (in a beaker) under vigorous stirring for 10 h. Then, 2 mmol CaCl<sub>2</sub> (dissolved in 10 mL de-ionized beforehand) was added into above clear solutions drop by drop. After about 15 min, the white precipitate appeared. Afterward, the beaker was covered with a glass dish and heated to 80 °C keeping for 12 h to complete the exchange of Na<sup>+</sup> by Ca<sup>2+</sup>. The precipitate was filtered and washed with water several times. Finally, Ca<sub>2</sub>BTEC was obtained by drying at 180 °C for 5 h. The synthesis procedure is shown in Scheme.1.



**Scheme.1** The synthesis procedure of Ca<sub>2</sub>BTEC by a hydrolysis and cationic exchange method

The phase composition and crystallinity of the as-prepared sample were characterised by powder X-ray diffraction (PXRD, MAXima-XXRD-7000). Fourier transform-infrared spectra analysis (FT-IR, Thermo Nicolet, 6700) was performed to further obtain the information of functional groups. The thermal stability of the sample was evaluated at a heating rate of 5 °C min<sup>-1</sup> from room temperature to 800 °C in air with a TG thermo-gravimetric analyzer

<sup>a</sup> Institute for Clean Energy & Advanced Materials, Faculty of Materials and Energy, Southwest University, Chongqing 400715, P.R. China

<sup>b</sup> Chongqing Key Laboratory for Advanced Materials and Technologies of Clean Energies, Chongqing 400715, P.R. China

<sup>c</sup> Key Laboratory of Advanced Energy Materials Chemistry (Ministry of Education), Nankai University, Tianjin 300071, China

\* Corresponding author

Fax: +86-23-68254969; Tel: +86-23-68254969;

E-mail: xumaowen@swu.edu.cn

† Electronic supplementary information (ESI) available. See DOI:

(TGA, TA Instruments Q50). For electrochemical testing, the anode materials were evaluated in 2032-type coin cells using a Na disk as the counter electrode and 1 M NaClO<sub>4</sub> in ethylene carbonate/diethyl carbonate (EC/DEC, 50 : 50 vol %) solution as the electrolyte. The anode electrodes were prepared by mixing the composite of active material (60 wt %), Super P carbon black (30 wt %) and carboxymethyl cellulose (CMC, 10 wt %) and dispersing in de-ionized water to form an electrode slurry. Then the slurry was casted onto a copper foil collector and dried overnight in a vacuum at 120 °C to remove the dispersant. The typical loading of active materials per electrode was approximately 1.5-2 mg. Assembly of the cells was carried out in a dry Ar-filled glove box (DELLIX, LS800S). Galvanostatic charge–discharge tests were performed on a LAND cyler (Wuhan Kingnuo Electronic Co., China). Cyclic voltammetry (CV) was performed at a scan rate of 0.1 mV s<sup>-1</sup> on an Arbin battery testing system. Electrochemical impedance spectroscopy (EIS) experiments were conducted in the frequency range of 0.1–100 kHz with a CHI600D electrochemical workstation.

Fig 1(a) displays the PXRD pattern of the as-prepared Ca<sub>2</sub>BTEC. All main X-ray diffraction peaks are sharp and strong, which indicates the as-prepared samples with high phase crystallinity. The PXRD pattern of Ca<sub>2</sub>BTEC is different from that of Ca<sub>2</sub>BTEC • 6H<sub>2</sub>O (CCDC No.1279417, Fig.S1), which can be attributed to that removing coordinated water causes some distortion in lattices.<sup>17, 18</sup> The crystal structure of Ca<sub>2</sub>BTEC is schematically shown in Fig 1(b). The connection of Ca<sup>2+</sup> with [C<sub>6</sub>H<sub>2</sub>(COO)<sub>4</sub>]<sup>4-</sup> forms obvious inorganic-organic hybrid layered structure, which is advantageous for the ex/insertion of Na<sup>+</sup>.<sup>19</sup>

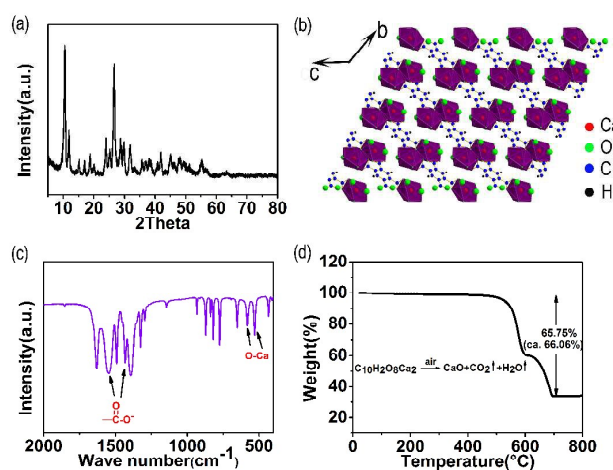


**Fig.1** (a) PXRD pattern, (b) crystal structure along *a*-axis, (c) FT-IR spectra and (d) TGA curve of the as-prepared Ca<sub>2</sub>BTEC.

In order to obtain the information of functional groups, FT-IR analysis was used. Fig 1(c) displays the FT-IR spectra of the as-prepared Ca<sub>2</sub>BTEC. The strong peaks located at 1650 cm<sup>-1</sup> and 1490 cm<sup>-1</sup> are assigned to symmetric and asymmetric carboxylate stretching vibrations, respectively. The relatively weak peaks between 600-400 cm<sup>-1</sup> are ascribed to the O-Ca bonds.<sup>20</sup> Above functional information can also prove the formation of a calcium-organic framework. Fig 1(d) shows the TGA curve of the synthesized sample. Below 500 °C, the quality of the sample is almost changeless, indicating the complete evaporation of coordinated

water during dry procedure and high thermal stability of Ca<sub>2</sub>BTEC. When heated from 500 °C to 800 °C, the sample shows a sharp weight loss of about 65.75% due to the pyrolysis from Ca<sub>2</sub>BTEC to CaO residues. The value of weight loss is almost consistent with the theoretical value according to reaction formula. Considering that water was used as solvent during electrode fabrication,<sup>21</sup> we further investigated the potential formation of Ca<sub>2</sub>BTEC • 6H<sub>2</sub>O. The TGA results in Fig S2 shows that the hydrated counterpart can not form during electrode fabrication procedure which ensures Ca<sub>2</sub>BTEC not Ca<sub>2</sub>BTEC • 6H<sub>2</sub>O as active material to participate in electrochemical reaction.

As a consequence of the unique inorganic-organic hybrid layered structure, Ca<sub>2</sub>BTEC exhibits excellent electrochemical performance as an anode material for SIBs. Fig 2(a) shows the discharge/charge voltage profiles of the as-prepared Ca<sub>2</sub>BTEC tested in the potential range 0.01-2.2 V and at a current density of 20 mA g<sup>-1</sup>. The first discharge capacity is 306 mA h g<sup>-1</sup>, while the charge capacity is only 140 mA h g<sup>-1</sup>. The initial capacity loss could be attributed to formation of SEI film on the electrode surface. Except the first cycle, a stable discharge/charge capacity of 120 mA h g<sup>-1</sup> can be attained. Similar voltage profiles can be found in sodium/lithium storage behaviour of TiO<sub>2</sub> and another MOF which indicates the reaction between Ca<sub>2</sub>BTEC and sodium species is a surface-confined charge-transfer process (pseudo-capacitive process).<sup>22-24</sup> A couple of broad redox peaks in CV curves (Fig. S3) also prove it. In addition, most of the discharge capacity is delivered below 1 V, which indicates a high output voltage of SIBs using prepared Ca<sub>2</sub>BTEC as anode materials.

The long-term cycle performance of Ca<sub>2</sub>BTEC is demonstrated in Fig 2(b). A superior high discharge capacity of 140 mA h g<sup>-1</sup> (86% of theoretical capacity) can be achieved after 300 cycles and the Coulombic efficiency is close to 100%. The excellent cycling capability can be attributed to the high structural stability (Fig.S4) and extremely low solubility (Fig.S5) of Ca<sub>2</sub>BTEC in the electrolytes.<sup>25</sup> Furthermore, Ca<sub>2</sub>BTEC electrode also shows a high rate capability up to 800 mA g<sup>-1</sup>. After discharged at 800 mA g<sup>-1</sup> for 5 cycles, the cell regains a capacity of 110 mA h g<sup>-1</sup> at 30 mA g<sup>-1</sup>, which also proves the high structural stability of Ca<sub>2</sub>BTEC. To further investigate the kinetics of the electrode process, Nyquist plots tested after different cycles are shown in Fig. 2(d). After 20 cycles, the R<sub>ct</sub> is about 2000 Ω. After 60 and 100 cycles, R<sub>ct</sub> decreases to 1000 Ω and 900 Ω, respectively, which can be ascribed to an electrochemical activation process.<sup>26</sup> The change of R<sub>ct</sub> is consistent with the capacity variation during long-term cycle test.

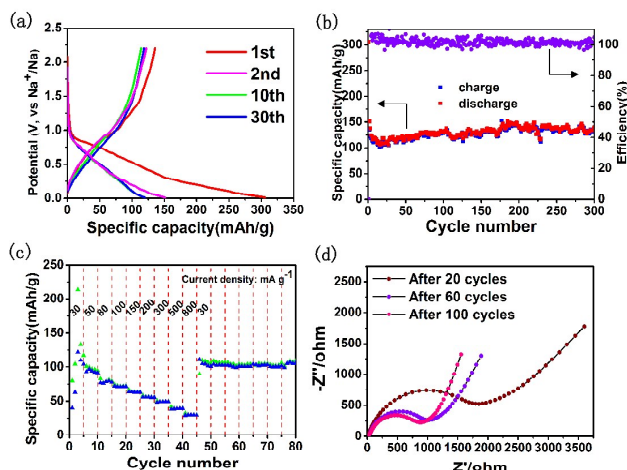


**Fig. 2** (a) Voltage profile at 20 mA g<sup>-1</sup> between 0.01-2.2 V versus Na<sup>+</sup>/Na; (b) long-term cycle performance at 20 mA g<sup>-1</sup>; (c) rate performance at different current density; (d) Nyquist plots before cycle test and after 20, 60, 100 cycles.

To explore the good electrochemical behaviour of Ca<sub>2</sub>BTEC, the de/sodiation mechanism is proposed in Fig 3. During sodiation, two C=O at the para-positions of one benzene ring are reduced to conjugated enol, which bond to two Na<sup>+</sup> ions. The reaction is a two-electron transfer reaction and offers a theoretical capacity of 162 mA h g<sup>-1</sup>. When desodiation, the conjugated enol could be reversibly oxidized to C=O with two electrons and Na<sup>+</sup> ions leaving. Similar mechanism could also be found in previous reports.<sup>27</sup> Compared with the poor electrochemical performance (Fig S7) of its hydrated counterpart (Ca<sub>2</sub>BTEC • 6H<sub>2</sub>O), it can be proposed that Ca<sub>2</sub>BTEC suffers weaker steric effect during de/sodiation due to removing coordinated water from inorganic-organic layered structure in synthesis procedure, which is more conducive and easier to the migration of Na<sup>+</sup>.

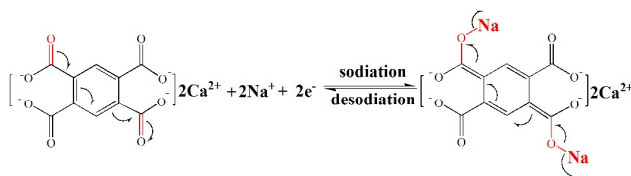


**Fig. 3** Proposed electrochemical redox mechanism of Ca<sub>2</sub>BTEC

## Conclusions

A novel Ca-based metal-organic framework was synthesized by a simple hydrolysis and cationic exchange reaction. Tested as an anode material for SIBs, it delivers a reversible capacity of 140 mA h g<sup>-1</sup> after 300 cycles and shows superior capacity retention and excellent rate performance. This work will further extend the family of anode materials for SIBs to more metal-organic frameworks.

## Acknowledgements

The work is supported by grants from Fundamental Research Funds for the Central Universities (SWU 113079, SWU 114099, XDJK2014C051, XDJK2015C062).

## Notes and references

- B. Dunn, H. Kamath and J.-M. Tarascon, *Science*, 2011, **334**, 928-935.
- K. B. Hueso, M. Armand and T. Rojo, *Energy Environ. Sci.*, 2013, **6**, 734-749.
- M. Xu, Y. Niu, C. Chen, J. Song, S. Bao and C. M. Li, *RSC Adv.*, 2014, **4**, 38140-38143.
- C.-Y. Yu, J.-S. Park, H.-G. Jung, K.-Y. Chung, D. Aurbach, Y.-K. Sun and S.-T. Myung, *Energy Environ. Sci.*, 2015, **8**, 2019-2026.
- Y.-U. Park, D.-H. Seo, H.-S. Kwon, B. Kim, J. Kim, H. Kim, I. Kim, H.-I. Yoo and K. Kang, *J. Am. Chem. Soc.*, 2013, **135**, 13870-13878.
- K. Saravanan, C. W. Mason, A. Rudola, K. H. Wong and P. Balaya, *Adv. Energy Mater.*, 2013, **3**, 444-450.
- M.-S. Balogun, Y. Luo, W. Qiu, P. Liu and Y. Tong, *Carbon*, 2016, **98**, 162-178.
- H. Hou, C. E. Banks, M. Jing, Y. Zhang and X. Ji, *Adv. Mater.*, 2015, **27**, 7861-7866.
- L. Liang, Y. Xu, C. Wang, L. Wen, Y. Fang, Y. Mi, M. Zhou, H. Zhao and Y. Lei, *Energy Environ. Sci.*, 2015, **8**, 2954-2962.
- Y. Liu, N. Zhang, L. Jiao, Z. Tao and J. Chen, *Adv. Funct. Mater.*, 2015, **25**, 214-220.
- Z. Song and H. Zhou, *Energy Environ. Sci.*, 2013, **6**, 2280-2301.
- C. Wang, Y. Xu, Y. Fang, M. Zhou, L. Liang, S. Singh, H. Zhao, A. Schöber and Y. Lei, *J. Am. Chem. Soc.*, 2015, **137**, 3124-3130.
- Z. Zhu, H. Li, J. Liang, Z. Tao and J. Chen, *Chem. Commun.*, 2015, **51**, 1446-1448.
- L. Wang, C. Mou, Y. Sun, W. Liu, Q. Deng and J. Li, *Electrochim. Acta*, 2015, **173**, 235-241.
- L. Wang, H. Zhang, C. Mou, Q. Cui, Q. Deng, J. Xue, X. Dai and J. Li, *Nano Res.*, 2015, **8**, 523-532.
- C. Mou, L. Wang, Q. Deng, Z. Huang and J. Li, *Ionics*, 2015, **21**, 1893-1899.
- A. S. Hameed, M. Nagarathinam, M. Schreyer, M. V. Reddy, B. V. R. Chowdari and J. J. Vittal, *J. Mater. Chem. A*, 2013, **1**, 5721-5726.
- A. S. Hameed, M. V. Reddy, M. Nagarathinam, T. Runčevski, R. E. Dinnebir, S. Adams, B. V. R. Chowdari and J. J. Vittal, *Sci. Rep.*, 2015, **5**.
- C. Robl, *Zeitschrift für Naturforschung B*, 1988, **43**, 993-997.
- M. Mazaj, G. Mali, M. Rangus, E. Žunkovič, V. e. Kaučič and N. a. Zabukovec Logar, *J. Phys. Chem. C*, 2013, **117**, 7552-7564.
- C. Wang, Y. Fang, Y. Xu, L. Liang, M. Zhou, H. Zhao and Y. Lei, *Adv. Funct. Mater.*, 2016, **26**, 1777-1786.
- G. Zou, J. Chen, Y. Zhang, C. Wang, Z. Huang, S. Li, H. Liao, J. Wang, and X. Ji, *J. Power Sources*, 2016, **325**, 25-34.
- Z. Hong, K. Zhou, J. Zhang, Z. Huang and M. Wei, *J. Mater. Chem. A*, 2015, **3**, 17412-17416.
- Y. Lin, Q. Zhang, C. Zhao, H. Li, C. Kong, C. Shen and L. Chen, *Chem. Commun.*, 2015, **51**, 697-699.
- T. Ma, Q. Zhao, J. Wang, Z. Pan and J. Chen, *Angew. Chem. Int. Ed.*, 2016, **55**, 6428-6432.
- L. Wang, Y. Yu, P. C. Chen, D. W. Zhang and C. H. Chen, *J. Power Sources*, **183**, 717-723.
- X. Wu, S. Jin, Z. Zhang, L. Jiang, L. Mu, Y.-S. Hu, H. Li, X. Chen, M. Armand and L. Chen, *Sci. Adv.*, 2015, **1**, e1500330.